RERTR 2022 – 42ND INTERNATIONAL MEETING ON
REDUCED ENRICHMENT FOR RESEARCH AND TEST REACTORS

OCTOBER 3-5, 2022
VIENNA INTERNATIONAL CENTRE
VIENNA, AUSTRIA

Forming Complex Nuclear Fuel Shapes in High-Loaded Silicide Surrogates

D.T. Clelland, D.R. Merkel, E.K. Nickerson, and K.P. Brooks,
V.V. Joshi, C.A. Lavender, Z.F. Huber
Pacific Northwest National Laboratory, 902 Battelle BLVD, 99352 Richland – USA

N. Carstens, and C. Mo
School of Engineering and Applied Sciences
Washington State University Tri-Cities, 2710 Crimson Way, 99354 Richland – USA

ABSTRACT

This work provides proof of the concept that high silicide loading nuclear fuel meat surrogates with complicated geometries can be produced with uniform density through an application of cold isostatic pressing (CIP). Dispersion fuels with high volumetric loading of U_3Si_2 have challenges in fabrication. Experimental work was undertaken using $MoSi_2$ and WSi_2 surrogates to explore the feasibility of reducing or eliminating the issues through the application of CIP in the powder compaction step. The composites were prepared at ~42 vol% silicide, which was representative of 4.8 gU/cc and formed via CIP at 50 ksi. The CIP mold design aimed to reduce defects and increase precision. The application of CIP here provides a strategy for producing highly loaded dispersion fuels with complex geometries and uniform density. The information associated with this document is preliminary, for information only, and should not be used as design input or operating parameters without user qualification.

1 Introduction

The traditional process for manufacturing dispersion nuclear fuels is to start with mixing the powdered materials (uranium fuel and aluminum binder), followed by uniaxially pressing the powders into a solid geometry with curvature on one side, then assembling into fuel packets with a filler (sometimes containing burnable absorber) and cladding, and finally rolling into the geometry of the fuel plate [1]. This work focuses on an alternative manufacturing process for the pre-rolled fuel part. The pre-rolled fuel part will be hereinafter referred to as the "billet". The traditional manufacturing approach presents several challenges in fuel fabrication. First, geometric constraints of uniaxial pressing limit the feasible fuel shapes. For example, curvature on more than one surface may be desired but is not possible to produce without variations in fuel density [2].

Second, the large deformations produced by the rolling process introduce geometric defects in the fuel such as dog-boning [1]. The defects introduced by rolling may be minimized or eliminated by intelligent design of the fuel geometry to compensate for undesirable deformations. For example, dog-boning may be suitably resolved by introducing a taper at the fuel end, thereby reducing the abrupt transition in mechanical properties between the aluminum picture frame and composite fuel as the packet passes between the rolls. Therefore, the manufacturing process may be improved by introducing a powder compaction method capable of producing complex geometries with multiple curved surfaces and tapered ends while maintaining uniform density.

Cold isostatic pressing (CIP) applies hydrostatic pressure on all surfaces of a part without external heat sources. CIP has an advantage over uniaxial compression of the powders because it applies pressure uniformly on all surfaces, regardless of shape, and thus is more conducive to creating consistent density throughout the parts. This contrasts with uniaxially loading where dies typically have straight, coaxial walls and parallel top and bottom surfaces with limited curvature. Curved top or bottom surfaces produce areas of high/low compaction resulting non-uniform density in the part [2]. In practice, CIP of metal powders is done by filling a polymer mold with the metal powder and then sealing that mold with a durable and evacuated liquid-tight bag. The assembly is then immersed in a liquid-filled pressure vessel which is pumped up to a high-pressure.

The objective of this research was to demonstrate CIP as a viable approach to forming complex geometry with multiple faces of curvature in nuclear fuel surrogates of U_3Si_2 dispersed in an aluminum matrix. Loading equivalents of 4.8 grams of uranium per cubic centimeter of fuel plus matrix (gU/cc) are commonly discussed as potential uranium loadings for high performance research reactors. $MoSi_2$ and WSi_2 were used as surrogate materials for U_3Si_2 at 42 vol% loading in Al matrix, which is volumetrically equivalent to 4.8 gU/cc. Particle size distributions (PSD) of Al, $MoSi_2$, and WSi_2 powders were characterized, and flow characteristics of the powder blends were determined. The density and microstructure of specimens were characterized. The mold cavity was scaled to 1.16X of the targeted part dimensions to compensate for powder compaction during CIP. The 1.16X was experimentally determined to be the scale necessary to reach the targeted dimensions upon CIP, during which there is volumetric reduction of the loosely packed powder as it consolidates into a solid metal part. The 1.16X scale is approximate because the volumetric reduction during CIP is believed to be dependent on the powder composite's morphology and PSD. In this study, the PSD was undesirably variable and therefore there was some inconsistency in the optimal scaling factor to reach our targeted geometry. During decompression the mold exerted stress on the surrogate fuel part due to becoming locally adhered to the surface of the part. The mold design was optimized to minimize this stress and prevent the surrogate fuel part from fracturing upon decompression.

2 Methods

2.1 Powder Materials and Blending

Elemental Al, $MoSi_2$, and WSi_2 powders were purchased from Stanford Advanced Materials (Lake Forest, CA). PSD shown in Figure 1 was determined according to ASTM B214 in which 100 g samples were sifted through sieves ranging from 20 to 177 μm mesh size (ASTM E-11 US Mesh no. 80 to 635). Figures shown in the 635-mesh bar account for all particles (fines) that passed through mesh size 635 without further qualification of their sizes. Powder blends were mixed using a rotating ball mill with a steel ball milling media. Hall flow and tapped density of each powder blend was evaluated according to ASTM B213 and B527, respectively.

2.2 Mold Manufacturing

Elastomer molds were fabricated by casting with XIAMETER™ RTV-4230-E Silicone or various

polyurethanes by first modeling a mold negative in SolidWorks 3D modeling software and then 3D printing using the off-the-shelf Fused Deposition Modeling capability of the Original Prusa i3 MK3S+ 3D printer. Mold negatives were printed in commercially available Polylactic acid (PLA) 3D printing filament. Then the 2-part castable polymer was mixed, degassed in a vacuum oven, and poured into the mold negatives.

A brace used for holding molds in shape during CIP was 3D printed directly in polyethylene terephthalate glycol, which was chosen for its rigidity in comparison to XIAMETER™ RTV-4230-E Silicone and its strength in comparison to PLA. The mold and brace are shown in Figure 8.

2.3 Cold Isostatic Pressing

Specimens were CIP in the elastomer molds in an American Isostatic Press (Columbus, OH) system at pressures of 50 KSI. Each mold was filled with a charge of powder and lightly tapped to consolidate the powder. Filled molds were bagged, evacuated of air, and heat-sealed and placed into the CIP vessel. The CIP pump was turned off immediately upon reaching the target pressure and was depressurized to atmospheric pressure over approximately 30 minutes.

2.4 Microscopy

Scanning electron microscopy (SEM) was performed on individual powders to determine morphology and optical microscopy was performed on CIP specimens to determine morphology. Powder specimens were prepared by attaching a random sample of powder to a glass slide using double-sided carbon tape. CIP specimens were mounted in epoxy and metallurgically polished to reveal a cross-section.

Surface profiles of the cold isostatically pressed surrogate fuel geometries were gathered by 3D scanning using a Keyence Optical Profiler VR-5000 Series and compared to their targeted profiles using SolidWorks 3D modeling software. The 3D scans were digitally leveled to align the surface profiles with the target profiles. The mid-section of the model was taken to be 0 in the Y-direction and the left side of the model was taken to be 0 in the X-direction.

3 Results and Discussion

3.1 *Characteristics of Powders and Powder Blends*

Examples of particle size distribution of each powder species are shown in Figure 1.Each of the purchased orders of metal powders differed in terms of PSD. The particle size used will have significant impacts on the results found in terms of mechanical properties of the parts formed and density. The correlation between particle size of powders used in manufacturing and the strength of the parts manufactured has been explored before [3]. Although not the focus of this proceeding, it was noted that there was a strong negative correlation between average particle size and the integrity of parts which were cold isostatically pressed. In other words, the larger the average particle size of the powders, the more cracks seemed to be present in the parts after CIP. There also seemed to be a limit in size of aluminum powder which could be used at all. A particularly large sized aluminum powder would not create a solid part at all when CIP with MoSi2 or WSi_2 at 50 KSI.

MoSi2 were non-spherical throughout all particle sizes (Figure 2). MoSi2 particles were coarse with nodular surfaces at all particle sizes. Similar morphology was observed in WSi_2 particles along with angular faceted particles. In contrast, Al particles were spherical with relatively smooth surfaces.

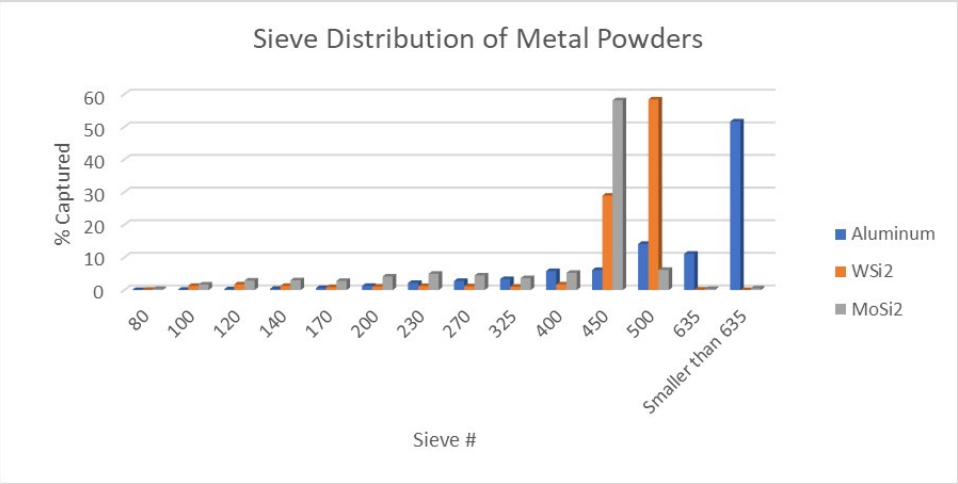

Figure 1. Examples of particle size distributions of the powders used.

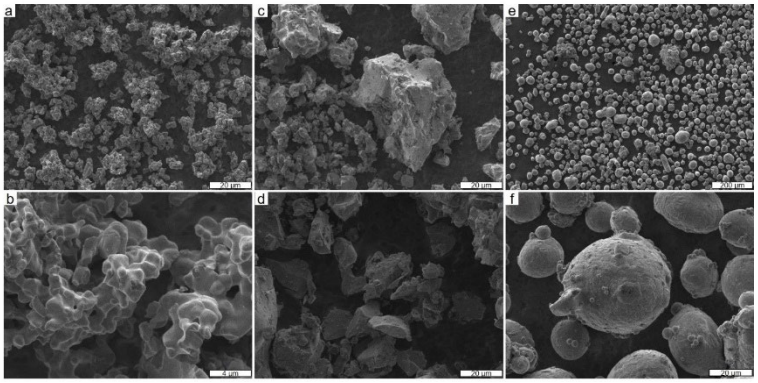

Figure 2. SEM micrographs of (a,b) $MoSi_2$ powder, (c,d) WSi_2 powder, and (e,f) Al powder. Note, micrographs of $MoSi_2$ and WSi_2 powders are represented at greater magnification compared to micrographs of Al powder to show particle morphology.

$MoSi_2$ and WSi_2 powders were blended with Al to match the volumetric proportions of 4.8 gU/cc U_3Si_2 + Al, which is 42 vol% silicide. This formulates to 63 mass % $MoSi_2$ and 72 mass % WSi_2. None of the powder blends flowed in Hall flow tests. Tapped densities were 1.95 g/cc and 3.41 g/cc for the $MoSi_2$–Al blend and WSi_2–Al blend, respectively.

3.2 *Characteristics of Cold Isostatic Pressed Specimens*

Optical micrographs of metallurgically polished specimens showed yielding of aluminum particles. The larger, relatively spherical aluminum particles yielded at point contacts with other aluminum particles or with silicide particles, which was evident at the perimeter of the aluminum particles. In contrast, yielding was not evident at point contacts between silicide particles. The yielding behavior is expected for the aluminum matrix particles at the pressures exerted during CIP due to the magnitudes far surpassing the yield and expected ultimate strengths of the aluminum. The WSi_2 and $MoSi_2$ were not expected to yield even at the highest CIP pressures. V-shell blenders likely work better to mix powders with large density differences as is the case with the materials in this work, but there appears to be a homogeneous mixture of the constituents in the surrogate billet once it has been pressed. See Figure 3.

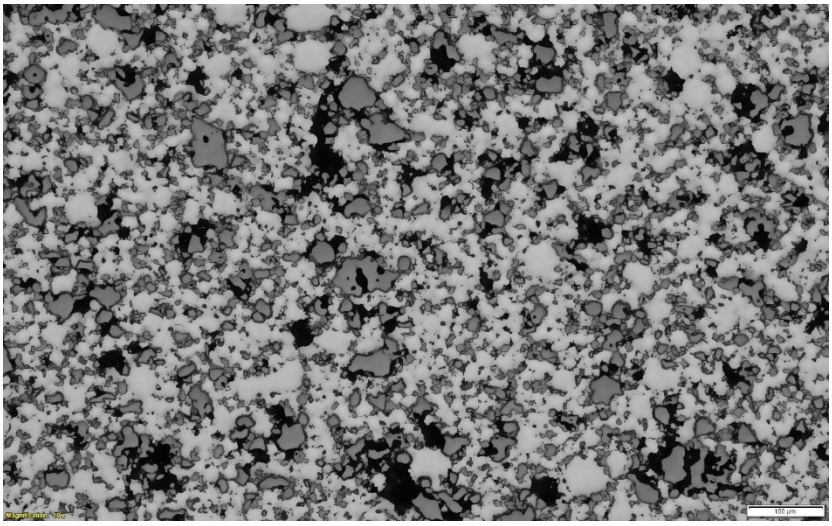

Figure 3. Optical microscopy of example $MoSi_2$ fuel geometry after 50 KSI CIP. The scale bar is 100um long.

CIP specimen density is known to depend on powder blend species, morphology, and particle size as well as pressing pressures. A CIP fuel geometry was examined for density uniformity by cutting the part into 9 approximately equal sized specimens for density measurement as shown in Figure 4 below. Each specimen was measured independently for density using ASTM Standard B962. The mean bulk density of these specimens was 4.096 g/cc with a standard deviation between the samples of 0.01345 g/cc. With a theoretical density of 4.210 g/cc, this gives an average part porosity of 2.7%. The porosity is equal to the theoretical density of a solid part minus the actual measured density divided by the theoretical density of a solid part.

The samples specifically mentioned in this paper are all $MoSi_2$ mixture parts, but that is just by happenstance of availability during certain times of testing. Although the 2 surrogates used in this work differed in morphology depicted here, and have a significant difference in density, when mixed in identical volume fraction (42%) with aluminum, there were no notable behavioral differences in CIP observed. This may bode well for this work's relevance to U_3Si_2 fuel manufacturing because of the similarity in pressing behavior between the two surrogate mixtures despite some differences in the properties of the silicide's.

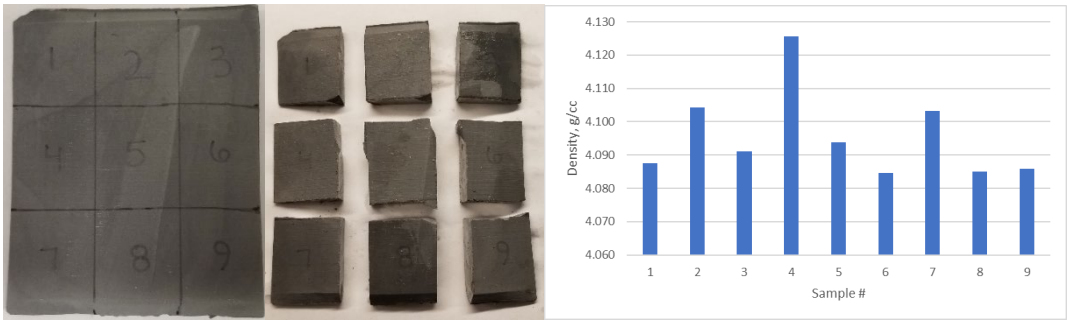

Figure 4. 50 KSI CIP fuel geometry partitioned prior to cutting, after being cut, density distribution according to ASTM Standard B962.

3.3 Mold Design

During this study, many iterations of mold design were used, including changes in geometry and material. A "clamshell" mold design example is shown in Figure 5. Both XIAMETER RTV-4230-E silicone and various polyurethanes were explored. Different mold materials were explored to reduce the number of cracked parts.

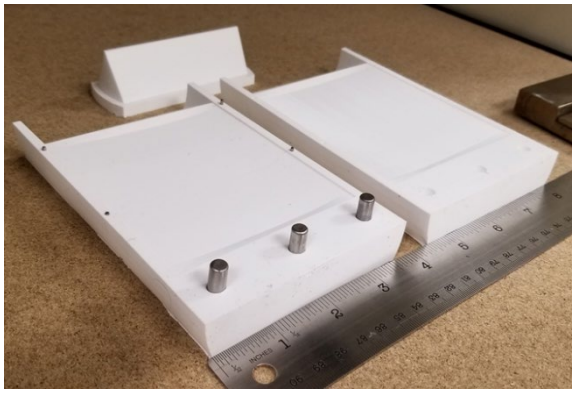

Figure 5. "clamshell" mold design example.

Figure 6. CIP fuel geometry parts which were cracked upon removal from CIP.

It is believed that the cause of the cracking in the parts was force exerted on the part by the mold during and after decompression (Figure 6). It is hypothesized that under high hydrostatic pressure of the CIP, the soft mold material was extruded between particles near the interface and adhered to the deformed and bonded particles by mechanical interlock. On decompression, the soft mold expanded elastically back to its original form while the part retained its condensed shape, inducing stress in the part at the interlocked surface. The parts adhered to the mold material and required gentle peeling to separate the mold from the part. Mold release agents were ineffective at reducing adhesion. Polyurethane molds with high durometer were also investigated to reduce interlock/adhesion without success. Polyurethane molds were abandoned due to the greater difficulty of casting compared to silicone.

Attempts were made to reduce the maximum elastic forces the mold could exert on the part through other means than reducing the adhesion between the mold and the part. This was done by reducing the thickness of the mold component which holds the metal powder, thereby reducing the amount of stored elastic energy which acts on the part during decompression. This concept was first implemented on a mold which had only ½ of the targeted geometry as shown in Figure 7. This was simpler to fill than a full-sized billet mold of the same design yet provided proof of concept that the reduction of mass of silicone which could act elastically on the part upon decompression reduced the frequency of fracture in the parts.

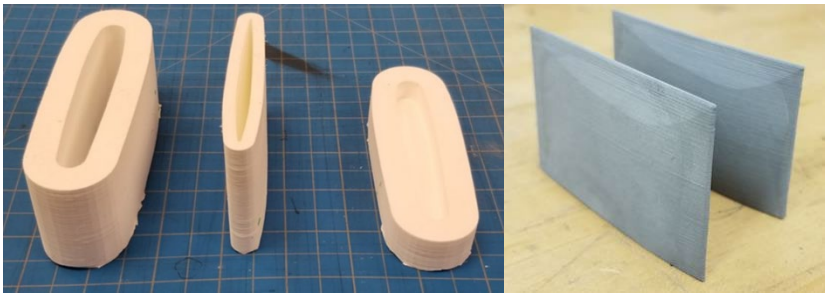

Figure 7. (Left) Half-size mold with thin inner mold cavity bag. (Right) two half geometry parts after release from molds.

Later a mold was created which included the entire target geometry's cavity (Figure 8) and implemented the same basic mold design which had a thin bag that contained the powder and was less able than the fully connected silicone design to exert elastic forces on the newly formed solid parts following decompression.

The mold opening where the powder is inserted has essentially zero-width. Therefore, it must be opened to receive the powder and then closed. The loose powder in the mold cavity must then be manipulated from the outside of the mold for it to closely conform to the targeted geometry. This practice of repositioning the powder after it is inside the mold has been conducted with only marginal success. The parts that have been made with this procedure have had defects of irregular width and also overall curvature of the billet. To apply pressure which would tend to hold the mold and powder assembly in its targeted orientation during CIP, a stiff brace was manufactured by 3D printing which would fit in the 3" diameter CIP and be able to survive the pressurized water environment for repeated use. The brace helped to reduce the magnitude of the irregular thickness of the billets produced but they were still present. While the overall curvature defect has been completely remedied.

Figure 8. (Left) Full-size billet geometry mold with brace disassembled. (Right) Full fuel geometry mold assembled with brace disassembled.

3.4 *CIP Geometries Optimization*

In Figures 9 and 10 the cross sections shown were compared to the targeted model geometry. Figure 9 compares cross sections in a part which was made by over filling the mold. Figure 10 shows a specimen which was made by filling the CIP mold to match its volume with tapped powder. This was done by establishing the tap density of the powder and then adding the appropriate mass to the mold based on its volume according to the SolidWorks model. The overfilled mold part has a shape which more closely resembles the target than the volume-matched, although its absolute dimensions are further off. The volume-matched part has a sinking defect towards the middle of each of the cross sections which is absent or less prevalent in the overfilled

mold part. For reference and to aid in comprehension of the profile comparisons, photographic images of the specimen from Figure 9 are given in Figures 11 and 12.

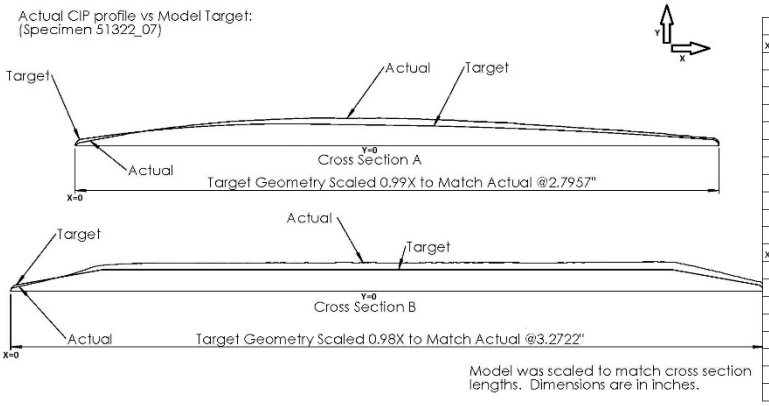

Cross Section A			
x	y-target	y-actual	error
0.0263	0.0273	0.0135	-0.0138
0.2501	0.0565	0.0545	-0.002
0.61	0.0859	0.0979	0.012
0.9699	0.0937	0.1164	0.0227
1.6897	0.0811	0.1064	0.0253
2.0496	0.0683	0.0852	0.0169
2.4095	0.0497	0.0615	0.0118
2.7696	0.0253	0.0321	0.0068
Cross Section B			
x	y-target	y-actual	error
0.0216	0.0267	0.017	-0.0097
0.4252	0.0931	0.1149	0.0218
0.8288	0.0931	0.1218	0.0287
1.2325	0.0931	0.1222	0.0291
1.6361	0.0931	0.1227	0.0296
2.4433	0.0931	0.124	0.0309
2.847	0.0931	0.1264	0.0333
3.2506	0.0267	0.0421	0.0154

Figure 9. Surface profile comparisons between target geometry and actual CIP geometry with overfilled mold cavity. Target geometry was slightly scaled for comparative purposes.

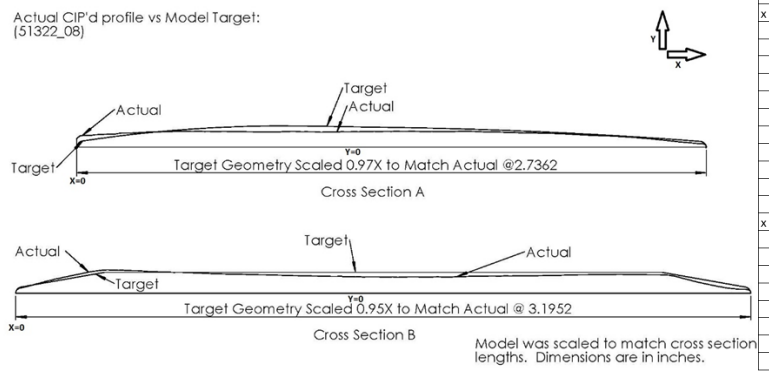

Cross Section A			
x	y-target	y-actual	error
0.0263	0.0268	0.0503	0.0235
0.4097	0.0715	0.067	-0.0045
0.793	0.0909	0.0658	-0.0251
1.1764	0.0884	0.066	-0.0224
1.5598	0.0818	0.0667	-0.0151
1.9431	0.0695	0.0609	-0.0086
2.3265	0.0505	0.0479	-0.0026
2.7099	0.0248	0.0155	-0.0093
Cross Section B			
x	y-target	y-actual	error
0.0216	0.0262	0.0234	-0.0028
0.4719	0.0909	0.0994	0.0085
0.9222	0.0909	0.0828	-0.0081
1.3725	0.0909	0.0723	-0.0186
1.8228	0.0909	0.0709	-0.02
2.273	0.0909	0.0762	-0.0147
2.7233	0.0909	0.0798	-0.0111
3.1736	0.0269	0.0165	-0.0104

Figure 10. Surface profile comparisons between target geometry and actual CIP geometry with powder volume-matched mold cavity. Target geometry was slightly scaled for comparative purposes.

Figure 11. Isometric view of example specimen.

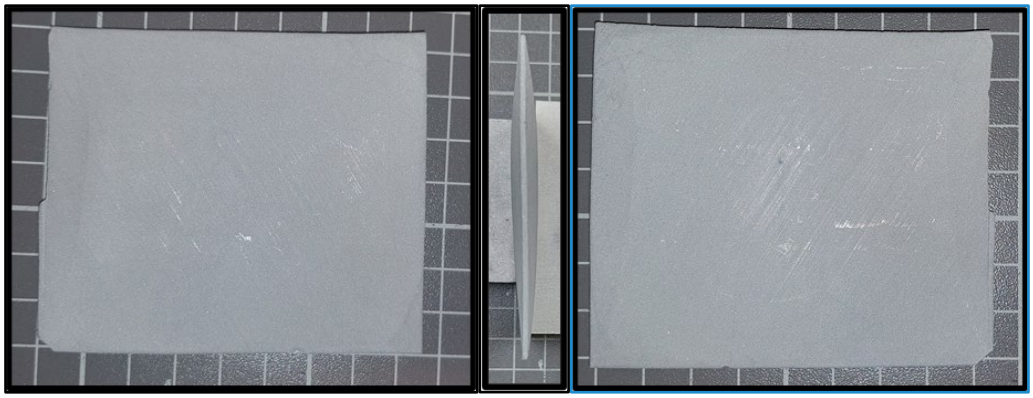

Figure 12. Left, top, and right views of example specimen (From left to right).

4 Conclusions

The study shows that there is promise in creating complex geometry dispersion fuel billets manufactured from U_3Si_2 and aluminum powders through CIP. This conclusion is derived from the uniform density found in the complex geometry of a part pressed by CIP using aluminum powder and $MoSi_2$ powder as a surrogate for U_3Si_2. This is contrasted with the traditional manufacturing method of uniaxial pressing of dispersion fuels, which is ineffective at producing uniform density parts in metal matrix composites with complex geometry.

Geometries which allow for a wide opening in the mold may be easier to manufacture due to ease of loading powder. A wide opening in the mold also eliminates the need to manipulate the mold and powder back into targeted geometry after elastically deforming it during the filling process. There is some benefit to using a hard brace to manipulate the mold and powder back into shape after deforming it during loading if necessary.

Further study of this work should examine optimizing the mold design to match the targeted geometry more precisely. Since it appears there is some improvement to the shape of the contours by over filling the mold, there should be a study done on optimizing the mold by designing it to be "overfilled" and go into a state of tension caused by the support of the powder. The deformations should also be studied and the feasibility of compensating in the geometry of the mold design to eliminate them should be explored. None of the powder blends flowed during Hall flow analysis, which may have negative implications for properly filling molds in a future automated process. A decrease in powder angularity or spherical powder could increase flow. Powder morphology and PSD have an impact on CIP results and would need to be held constant to produce consistent fuel parts through CIP manufacturing.

5 References

[1] Durazzo, M., et al. "Evolution of fuel plate parameters during deformation in rolling." *Journal of Nuclear Materials* 490 (2017): 197-210. https://doi.org/10.1016/j.jnucmat.2017.04.018

[2] Doyle LE. Manufacturing Processes and Materials for Engineers. 2nd ed. Englewood Cliffs N.J: Prentice-Hall; 1969.

[3] Lin, Ching-Shan, and Shun-Tian Lin. "Effects of granule size and distribution on the cold isostatic pressed alumina." *Journal of Materials Processing Technology* 201.1-3 (2008): 657-661. https://doi.org/10.1016/j.jmatprotec.2007.11.159